Dimensionless Analysis of the Simulation of Bucket Foundations under Dynamic Load

Xuhui Zhang* Xiaobing Lu and Shuyun Wang

Institute of Mechanics, Chinese Academy of Sciences, 100190, Beijing, China

Abstract: Firstly, the main factors are obtained by use of dimensionless analysis. Secondly, the time scaling factors in centrifuge modeling of bucket foundations under dynamic load are analyzed based on dimensionless analysis and controlling equation. A simplified method for dealing with the conflict of scaling factors of the inertial and the percolation in sand foundation is presented. The presented method is that the material for experiments is not changed while the effects are modified by perturbation method. Thirdly, the characteristic time of liquefaction state and the characteristic scale of affected zone are analyzed.

Keywords: Dynamic load, bucket foundation, centrifugal experiment, time scale.

INTRODUCTION

A suction bucket foundation is a closed-top steel tube that is lowered to the seafloor, allowed to penetrate the bottom sediments under its own weight, and then pushed to full depth with suction force produced by pumping water out of the interior. In recent years, suction bucket foundations have been used increasingly for gravity platform, jackets, jack-ups etc. [1, 2]. They also have the potential of being used for several other purposes, such as offshore wind turbines, subsea systems and seabed protection structures [3-6]. The first advantage of suction bucket foundation is the convenient installation and reusability. For example, a suction bucket foundation with a diameter of 9m and a height of 10m can be installed in 1~3 hours, only by using a pump. The second advantage is that it may mobilize a significant amount of passive suction during uplift under some conditions, although the mobilization of suction depends mainly on the load rate and recommendations are actually to not rely on the suction for design [7]. Despite studies of the installation and bearing capacity, the detail responses of the suction bucket foundations under dynamic loads remain unknown [8-10]. The dynamic load condition is significant when suction buckets are used as the foundation of an offshore structure. Wave load, ice-induced or wind-induced load cause the foundation to suffer cyclic loads [11, 12]. This requires a test program to gain a deeper understanding. Prototype tests need considerable expense and time. Thus they are unpractical. But it is much easier to change parameters in small scale tests. The soil type may be varied in these cases. The dimensions of the suction bucket and other process parameters may be varied conveniently also. Nevertheless, in a small scale test, the problems arise concerning the stress-dependent behavior of soil that the measured loads are so low that measurements are not sufficiently accurate to visualize differences in design. Because the soil behavior depends on stress, small scale model tests can not exhibit the same responses. These restrictions can be overcome by tests in a geotechnical centrifuge. Centrifugal tests are "model" tests in that the results can be scaled up to the size of full-scale buckets. The main reason to select centrifugal test is for the proper modeling of body forces, which are critically important for the full-scale prototype geotechnical problem, and for the capability of investigating both undrained and partially drained conditions.

The scaling law is very important in centrifugal experiments. Especially the conflict time scaling factors should be considered if the problem is related to the consolidation and dynamic load.

In this paper, dimensionless analysis is used to obtain the main factors affected the dynamic responses of the bucket and the soil layer surrounding the bucket. Some characteristic parameters, such as the time to arrive at the liquefaction state and the characteristic scale of affected zone, are obtained by theoretical analysis. The theoretical results are compared with the centrifugal experimental results.

DIMENSIONLESS ANALYSIS

The Scaling Analysis

Dimensionless analysis is often used for simplifying experiments and numerical simulations, and also for obtaining the main factors.

The controlling factors here include the parameters of soils, pore water, bucket and load.

(1) The parameters of soils: multilayered soils have a set of parameters for each layer. For convenience, we list the parameters of one layer: the density ρ_s, porosity n, elastic modulus E and the poisson's ratio ν. Here we adopted the

*Address correspondence to this author at the Institute of Mechanics, Chinese Academy of Sciences, 100190, Beijing, China; Tel: 861082544192; E-mail: zxh424@163.com

1874-835X/10

plastic hardening index H_p and the plastic proportional load coefficient λ_p to describe the plastic responses. Assuming the soil layer satisfies the Mohr-Column criterion, which means, the strength of soils may be expressed as $\tau_f = c + \sigma \tan\varphi$. Thus, the parameters of strength include the cohesion c and the internal friction angle φ. The other parameters include the thickness of soil layer h and the physical permeability K.

(2) The parameters of water: density ρ_w, viscosity coefficient μ, depth h_w.

(3) The parameters of bucket: diameter D, height H, thickness d, elastic modulus E, poisson's ratio ν_s and density ρ. In practice, the bucket is difficult to be made as the scaled value for the thickness is too small, and the structural property may change because of the size effect. Generally, we deal it in this way: ensure the similarity of the inertial and the bending moment since the material strength of the bucket is much bigger than that of the soil layers and only small elastic deformation occurs in buckets. Then the controlling parameters are as follows: total mass M, total bending moment $J = EI$ in which I is the inertial moment. At the same time, the diameter of the bucket D, the height H and the friction angle between the bucket and the soil θ should be considered. Thus, the parameters of bucket are D, H, M, J, θ, respectively.

(4) The load parameters: the amplitude F, frequency f, duration T, horizontal static load F_h, vertical static load F_v and the gravity acceleration g.

The viscosity of water μ and the physical permeability K is always combined K/μ to describe as the interaction between the pore water and the grains. The function of interaction between the pore water and the grains is $f_c = \frac{K}{\mu} n^2 (u_s - u_w)$, in which u_s, u_w are the velocities of grains and pore water, respectively.

The unknowns are the bearing capacity P_1, displacement of bucket U and the pore pressure p. The relations between the controlling factors and the unknowns can be expressed as:

$$\begin{matrix} P_l \\ U \\ p \end{matrix} = f\begin{pmatrix} \rho, n, E_s, \nu_s, h_p, \lambda_p, c, \varphi, h, \rho_w, \\ \\ k/\mu, h_w, D, H, M, J, \theta, F, f, T, F_h, F_v, g \end{pmatrix}$$

Choosing the diameter of bucket D, density of soil ρ_s and the gravity acceleration g as the basic parameters, we can rewrite the above relation in dimensionless form:

$$\begin{matrix} \frac{P_l}{\rho_s g D^3 \tan\varphi} \\ \frac{U}{D} \\ \frac{p}{\rho_s g D \tan\varphi} \end{matrix} = f\begin{pmatrix} n, \frac{E_s}{\rho_s g D}, \nu_s, \frac{h_p}{\rho_s g D}, \lambda_p, \frac{c}{\rho_s D g}, \varphi, \frac{\rho_w}{\rho_s}, \frac{k\rho_s D}{\mu} \\ \frac{h_w}{D}, \frac{H}{D}, \frac{M}{\rho_s D^3}, \frac{J}{\rho_s g D^5}, \theta, \frac{F}{\rho_s g D^3 \tan\varphi}, \frac{f}{\sqrt{g/D}}, \\ T\sqrt{g/D}, \frac{F_h}{\rho_s g D^3 \tan\varphi}, \frac{F_v}{\rho_s g D^3 \tan\varphi} \end{pmatrix}$$

Generally, the percolation is related closely to the load frequency. The high the load frequency, the lower the percolation is. Thus the above equation can be rewritten as:

$$\begin{matrix} \frac{P_l}{\rho_s g D^3 \tan\varphi} \\ \frac{U}{D} \\ \frac{p}{\rho_s g D \tan\varphi} \end{matrix} = f\begin{pmatrix} n, \frac{E_s}{\rho_s g D \tan\varphi}, \nu_s, \frac{h_p}{\rho_s g D}, \lambda_p, \frac{c}{\rho_s D g}, \varphi, \frac{\rho_w}{\rho_s}, \frac{k\rho_s\sqrt{gD}}{f\mu}, \frac{h_w}{D}, \frac{H}{D}, \\ \frac{M}{\rho_s D^3}, \frac{J}{\rho_s g D^5 \tan\varphi}, \theta, \frac{F}{\rho_s g D^3 \tan\varphi}, \frac{f}{\sqrt{g/D}}, T\sqrt{g/D}, \frac{F_h}{\rho_s g D^3 \tan\varphi}, \\ \frac{F_v}{\rho_s g D^3 \tan\varphi} \end{pmatrix}$$

In the above formula, there are 19 dimensionless parameters:

n indicates the porosity of soils.

$\frac{c_i}{\rho_s D g}$: the relative cohesion

φ : the internal friction angle

$\frac{E_s}{\rho_s g D}$: the dimensionless soil modulus

ν_s : the soil poisson's ratio

$\frac{h_p}{\rho_s g D}$: the dimensionless hardening index of soils

λ_p : the plastic proportional load coefficient

$\frac{\rho_w}{\rho_s}$: the relative density

$\frac{k\rho_s\sqrt{gD}}{f\mu}$: the dimensionless permeability

$\frac{h_w}{D}$: the relative water depth

$\frac{H}{D}$: the height-to-diameter ratio

$\frac{M}{\rho_s D^3}$: the relative mass between bucket and the effected soils

$\frac{J}{\rho_s g D^5}$: the dimensionless bending moment

θ : the friction between the bucket and the soils

$\frac{F}{\rho_s g D^3 \tan\varphi}$: the ratio of load amplitude to anti-force of soil layer

$\frac{f}{\sqrt{g/D}}$: the dimensionless load frequency

$T\sqrt{g/D}$: the relative action duration of load

$\frac{F_h}{\rho_s g D^3 \tan\varphi}, \frac{F_v}{\rho_s g D^3 \tan\varphi}$: the ratio of horizontal static load to the anti-force of soils and the ratio of vertical static load to the anti-force of soils, respectively.

Similarity of Geometry

According to the analysis above, it is easy to see that in experiments, the scaling laws of suction bucket foundations under dynamic load are difficult to satisfy fully. That means, if only the size of geometry changes while the materials does not changes, not all similar parameters can be satisfied, except for the experiments of full size. Nevertheless, it can be solved partly if centrifugal experiments are adopted. In centrifugal experiments, $a_m = Ng_p$, a_m is the centrifugal acceleration, g_p is the acceleration in prototype, $L_m = \frac{1}{N} L_p$, L is a length. Assuming that the materials (soils and water) do not change, the similarity conditions are as follows:

$$\begin{matrix} \frac{P_l}{\rho_s g D^3 \tan\varphi} \\ \frac{U}{D} \\ \frac{p}{\rho_s g D \tan\varphi} \end{matrix} = f \begin{pmatrix} n, \frac{c}{\rho_s D^{1.5} g^{0.5}}, \varphi, \frac{E_s}{\rho_s g D \tan\varphi}, \nu_s, \frac{h_p}{\rho_s g D \tan\varphi}, \lambda_p, \\ \frac{\rho_w}{\rho_s}, \frac{k\rho_s\sqrt{gD}}{f\mu}, \frac{h_w}{D}, \frac{H}{D}, \frac{M}{\rho_s D^3}, \frac{J}{\rho_s D^6}, \frac{F}{\rho_s g D^3 \tan\varphi}, \\ \frac{f}{\sqrt{g/D}}, T\sqrt{g/D}, \frac{F_h}{\rho_s g D^3 \tan\varphi}, \frac{F_v}{\rho_s g D^3 \tan\varphi}, \theta \end{pmatrix}$$

in which the similar relations are as follows: $n_m = n_p$, $\varphi_m = \varphi_p$, $\left(\frac{E_s}{E}\right)_m = \left(\frac{E_s}{E}\right)_p$, $\nu_{sm} = \nu_{sp}$, $\left(\frac{h_p}{\rho_s g D \tan\varphi}\right)_m = \left(\frac{h_p}{\rho_s g D \tan\varphi}\right)_p$, $\lambda_{pm} = \lambda_{pp}$, $\left(\frac{\rho_w}{\rho_s}\right)_m = \left(\frac{\rho_w}{\rho_s}\right)_p$, $\left(\frac{H_w}{D}\right)_m = \left(\frac{H_w}{D}\right)_p$, $\left(\frac{H}{D}\right)_m = \left(\frac{H}{D}\right)_p$. The above parameters are satisfied naturally. The following relations should be scaled: $\left(\frac{c}{\rho_s}\right)_m = \frac{1}{N}\left(\frac{c}{\rho_s}\right)_p$, $\left(\frac{k\rho_s}{f\mu}\right)_m = \left(\frac{k\rho_s}{f\mu}\right)_p$, $M_m = \frac{1}{N^3} M_p$, $J_m = \frac{1}{N^5} J_p$, $F_m = \frac{1}{N^2} F_p$, $f_m = N f_p$, $T_m = \frac{1}{N} T_p$, $F_{hm} = \frac{1}{N^2} F_{hp}$, $F_{vm} = \frac{1}{N^2} F_{vp}$. The following relation is difficult to satisfy:

$\left(\frac{k\rho_s}{f\mu}\right)_m = \left(\frac{k\rho_s}{f\mu}\right)_p$. In other words, although the similarity of gravity may be satisfied in centrifugal experiments, the similarity law of geometry can not be satisfied.

The Method for Simplifying the Controlling Parameters

Momentum equilibrium equation are as follows:

$$\begin{cases} \frac{\partial \sigma_{ij}}{\partial x_j} - \frac{\partial p}{\partial x_i} = (1-\varepsilon)\rho_s \frac{\partial^2 u_i}{\partial t^2} + \varepsilon\rho \frac{\partial v_i}{\partial t} \\ -\frac{\partial p}{\partial x_i} - \frac{\varepsilon\mu}{K}(v_i - \frac{\partial u_i}{\partial t}) = \rho \frac{\partial v_i}{\partial t} \end{cases} \quad (1)$$

Mass equilibrium equation

$$\begin{cases} \frac{\partial \varepsilon\rho}{\partial t} + \varepsilon\rho \frac{\partial v_i}{\partial x_i} = 0 \\ \frac{\partial (1-\varepsilon)\rho_s}{\partial t} + (1-\varepsilon)\rho_s \frac{\partial^2 u_i}{\partial t \partial x_i} = 0 \end{cases} \quad (2)$$

Constitutive relation

$$\sigma_{ij} = G(\frac{\partial u_i}{\partial x_j} + \frac{\partial u_j}{\partial x_i}) + \delta_{ij} \frac{2G\nu}{1-2\nu} \frac{\partial u_k}{\partial x_k} \quad (3)$$

in which ρ is the pore fluid density, ρ_s is the skeleton density, u_i is the skeleton velocity, v_i is the pore fluid velocity, p is the pore pressure, σ_{ij} is the effective stress, g is the gravity acceleration, G is the shear modulus, ν is the poisson's ratio.

The stream function and potential function are introduced in the following analysis:

$$\begin{cases} \bar{u} = Grad\varphi_s + Curl\bar{\psi}_s \\ \bar{v} = Grad\varphi + Curl\bar{\psi} \\ Div\bar{\psi}_s = 0 \\ Div\bar{\psi} = 0 \end{cases} \quad (4)$$

Instituting eq.(4) into eqs.(1)~(3), yields

$$\frac{2G(1-\nu)}{\rho_s(1-2\nu)}\nabla^2\varphi_s = \frac{\mu\omega}{\rho_s K}\left[\frac{\partial\varphi_s}{\partial\tau} + \frac{\omega\rho_s K}{\mu}(1-\varepsilon)(1+\frac{1-\varepsilon}{\varepsilon}\frac{\rho}{\rho_s})\frac{\partial^2\varphi_s}{\partial\tau^2}\right] \quad (5)$$

and

$$\frac{G}{\rho_s}\nabla^2\bar{\psi}_s = \omega^2\left(1-\varepsilon+\frac{\varepsilon\rho}{\rho_s}\right)\frac{\partial^2\bar{\psi}_s}{\partial t^2} \quad (6)$$

in which $\tau = \omega t$, ω is the load frequency.

It can be seen that $\eta = \omega\rho_s K/\mu$ is a small parameter in this problem. The multi-scale asymptotic expansions method is used here, which is

$$\begin{cases} \varphi_s = \varphi_s^0(x_i,\tau_1,\tau_2) + \sum_{n=1}^{\infty}\eta^n\varphi_s^{(n)}(x_i,\tau_1,\tau_2) \\ \bar{\psi}_s = \bar{\psi}_s^0(x_i,\tau_1,\tau_2) + \sum_{n=1}^{\infty}\eta^n\bar{\psi}_s^{(n)}(x_i,\tau_1,\tau_2) \end{cases} \quad (7)$$

in which $\tau_1 = \tau, \tau_2 = \eta\tau$. Instituting eq. (7) into eqs. (5)~(6), we get

$$D\nabla^2\varphi_s^{(1)} = \frac{\partial\varphi_s^{(1)}}{\partial\tau} \tag{8}$$

$$D\nabla^2\varphi_s^{(n)} = \frac{\partial\varphi_s^{(n)}}{\partial\tau_1} + \frac{\partial\varphi_s^{(n-1)}}{\partial\tau_2} + (1-\varepsilon)\left(1+\frac{1-\varepsilon}{\varepsilon}\frac{\rho}{\rho_s}\right)\left(\frac{\partial^2\varphi_s^{(n-1)}}{\partial^2\tau_1} + \frac{\partial^2\varphi_s^{(n-2)}}{\partial\tau_1\partial\tau_2} + \frac{\partial^2\varphi_s^{(n-3)}}{\partial^2\tau_2}\right) \tag{9}$$

$$\lambda\nabla^2\overline{\psi}_s^{(0)} = \frac{\partial^2\overline{\psi}_s^{(0)}}{\partial\tau_1^2} \tag{10}$$

$$\lambda\nabla^2\overline{\psi}_s^{(1)} = \frac{\partial^2\overline{\psi}_s^{(1)}}{\partial\tau_1^2} + \frac{\partial^2\overline{\psi}_s^{(0)}}{\partial\tau_1\partial\tau_2} \tag{11}$$

$$\lambda\nabla^2\overline{\psi}_s^{(n)} = \frac{\partial^2\overline{\psi}_s^{(n)}}{\partial\tau_1^2} + \frac{\partial^2\overline{\psi}_s^{(n-1)}}{\partial\tau_1\partial\tau_2} + \frac{\partial^2\overline{\psi}_s^{(n-2)}}{\partial\tau_2^2} \tag{12}$$

in which $D = \frac{2GK(1-\nu)}{\mu\omega(1-2\nu)}$, $\varphi_s^{(0)} = 0$,

$\lambda = \frac{G}{\omega^2\left[(1-\varepsilon)\rho_s + \varepsilon\rho\right]}$.

It is shown that $\psi_s^{(0)}$ is the high frequency component (denoting the initial response). This component satisfies the wave motion and thus is a fast course. In the zero order, there are only shear waves. $\varphi_s^{(1)}$ is the low frequency component (denoting the percolation and consolidation). This component satisfies the disperse equation respecting the percolation and consolidation and thus is a slow course. It is shown that three dimensionless parameters must be satisfied if the geometrical similarity is satisfied: $\frac{\rho g L}{\sigma}$, $\frac{R}{\rho\omega^2 L^2}$ and $\frac{RK}{\mu\omega L^2}$, in which R denotes the stiffness of the system.

The method to solve the conflict of time scaling factors

Especially the conflict time scaling factors should be considered if the problem is related to the consolidation and dynamic load.

Consolidation relates to the dissipation of excess pore pressure and is a diffusion event. The velocity of consolidation is described by the dimensionless time T_v defined as: $T_v = \frac{c_v t}{H^2}$, where c_v is the coefficient of consolidation, t is the time and H is a length related to a drainage path. It is easy to obtain the scaling relation of consolidation as $t_m = \frac{1}{N^2}\frac{c_{vp}}{c_{vm}}t_p$. Hence, if the same material is used in model and prototype, the time scaling factor is $1:N^2$. If for some reason the permeability in model and prototype is different, the time scaling relation becomes: $t_m = \frac{1}{N^2}\frac{k_p}{k_m}t_p$, where k_p, k_m are the coefficients of permeability in model and prototype respectively [13].

For the case of dynamic load, it is easy also to obtained the scaling factors of linear dimension, acceleration and frequency: $1:N, 1:N^{-1}$. An important consequence is that the time scaling factor for dynamic events is $1:N$ in contrast to $1:N^2$ time scaling factor for diffusion or seepage events.

The conflict of time scaling factors requires special consideration when both the dynamic effect and the seepage are present. The method to ensure the same time scaling factor for motion and seepage is usually to decrease the effective permeability of solid material by increasing the viscosity of the pore fluid or by the changing the grain series of solid material.

If the material is not changed during centrifugal experiments, all parameters except $k\rho_s\sqrt{gD}/(f\mu)$ and $c/(\rho_s D^{1.5} g^{0.5})$ satisfy the scaling law. Therefore, it is the key problem to deal with the similar simulation of these two parameters for sand foundation. Now, we compare the characteristic time of the permeability, inertial and load duration.

Characteristic time of percolation is $\frac{\mu H^2}{KE(1+e)} \sim 10^6$, the load cycle is $\frac{1}{f} \sim 1.25$, the total load duration is $T \sim 10^7$. in which $K = 4\times10^{-12} m^2$, $E = 8\times10^6 Pa$, $H = 5m$, $g = 10 m/s^2$, $f = 0.8Hz$.

Now, it can be seen that: (1) The load cycle is small compared with the percolation characteristic time, thus the inertial movement and percolation can be decoupled. (2) The total load duration is bigger than that of the characteristic time of percolation and the load cycle when the frequency is relatively high. Thus the effects of percolation in the early stage are small. That is say, even if the permeability and the load cycle do not satisfy the scaling law fully, the final responses of soil layer and the pore water are still close to the real value which need only modified by perturbation method if the frequency is relatively large.

THE DURATION TO ARRIVE AT THE STABLE STATE UNDER DYNAMIC LOAD

Let Δ denotes the character displacement on the boundary, T the character time and L the character length. Thus the following equation may be obtained by eq. (5)

$$\frac{2G(1-\nu)}{\rho_s(1-2\nu)}\frac{T^2}{L^2}\frac{\rho_s K}{\mu T}\nabla^2\Phi_s = \frac{\rho_s K}{\mu T}(1-\varepsilon)(1+\frac{1-\varepsilon}{\varepsilon}\frac{\rho}{\rho_s})\frac{\partial^2\Phi_s}{\partial\tau^2}+\frac{\partial\Phi_s}{\partial\tau} \quad (13)$$

The wave velocity is

$$c = (a/b)^{0.5}$$

in which

$$a = \frac{2G(1-\nu)}{\rho_s(1-2\nu)}\frac{T^2}{L^2}\frac{\rho_s K}{\mu T},$$

$$b = \frac{\rho_s K}{\mu T}(1-\varepsilon)(1+\frac{1-\varepsilon}{\varepsilon}\frac{\rho}{\rho_s})$$

The affected zone can be determined by the following equation

$$\delta = \frac{c}{\omega} \quad (14)$$

In Fig. (**1**), the solid line is the theoretical value and the dots are experimental value. (according to the triaxial experiments and percolation tests, the modulus of soil layer is $E = 8MPa$, the permeability is $K = 2\times10^{-9} m^3 s/kg$, the frequency is $\omega = 1.26 \sim 7.85/s$.). It is shown that the experimental and theoretical results are agreement with each other.

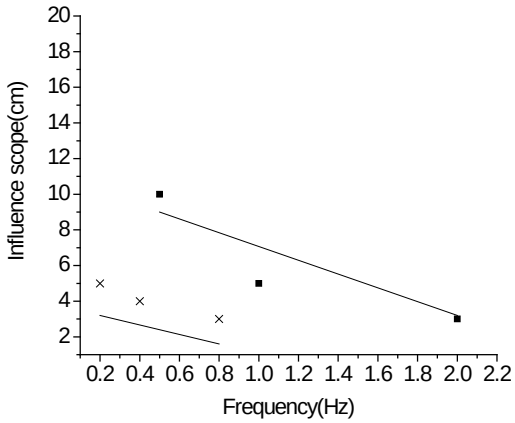

Fig. (1). Comparison of the theoretical and experimental results of effected zone under dynamic loadings.

(The block dots are obtained from centrifugal experiments, the other dots are obtained from small scale experiments.)

Now, we can solve the character time that arrives at the stable state. Assuming L is the character length, μ is the viscosity of water, k is the permeability, u is the character displacement, thus the pore pressure p, effective stress σ_e and inertial force σ_d can be expressed as $p = \frac{\mu L}{k}\dot{u}$, $\sigma_e = E\frac{u}{L}$, $\sigma_d = \frac{\rho L}{2}\ddot{u}$, respectively. $F(t)$ is the applied force. Therefore, the equilibrium equation of force can be expressed as follows:

$$\frac{\rho L}{2}\ddot{u}+\frac{\mu L}{k}\dot{u}+E\frac{u}{L} = F(t) \quad (15)$$

or

$$m\ddot{u}+C\dot{u}+Ku = F(t) \quad (16)$$

in which

$$m = \frac{\rho L}{2};\quad C = \frac{\mu L}{k};\quad K = \frac{E}{L}$$

The frequency is as follows at $F(t) = 0$

$$m\omega_0^2 - iC\omega_0 - K = 0 \quad (17)$$

$$\omega_0 = \frac{iC \pm \sqrt{-C^2+4mK}}{2m} = i\frac{\mu}{\rho k}(1 \pm \sqrt{1-2\rho E\frac{k^2}{\mu^2 L^2}}) \quad (18)$$

When $2\rho E\frac{k^2}{\mu^2 L^2}$ is enough small, the frequency may be written as

$$\omega_{01} = i\frac{2\mu}{\rho k};\quad \omega_{02} = iE\frac{k}{\mu L^2} \quad (19)$$

Therefore, the character time that arrives at stable state is: $\frac{\mu L^2}{Ek}$. According to the data in experiments, the theoretical time to arrive at stable state is about 2 hours which is close to the experimental value [6].

VERIFICATION

To verify the above theoretical results, experimental results are compared with that of theoretical results. First, the development of the excess pore pressure and the displacement of bucket with time are investigated, secondly, the time to arrive at the stable response state in experiments is compared with the theoretical value.

It is shown that from Figs. (**2**) and (**3**) the excess pore pressure increases to the maximum at the first stage once the load is applied and then decreases gradually to a relative stable state. The settlement of the bucket increases to the maximum gradually. It indicates that the responses of the bucket and the soil layer will arrive at a relatively stable state under long-term dynamic load. Figs. (**4**) and (**5**) show a planform and a section of affected zone after experiments. It is shown that there exists an affected zone with finite range under long-term dynamic load. The settlement and the density of soil increase inner the zone. The characteristics of the load and the permeability can only affect the midcourse of the bucket and the soil around the bucket, but not the final state.

Fig. (**6**) shows the comparison of development course of the pore pressure and the bucket's settlement. It is shown that the bucket settles small (20% of the total settlement) during the increase of pore pressure. The settlement of bucket increases to the maximum during the pore pressure decreases to the stable state. Therefore, only if the duration of load is enough, the settlement will develop to the maximum. The maximum of settlement does not change with permeability.

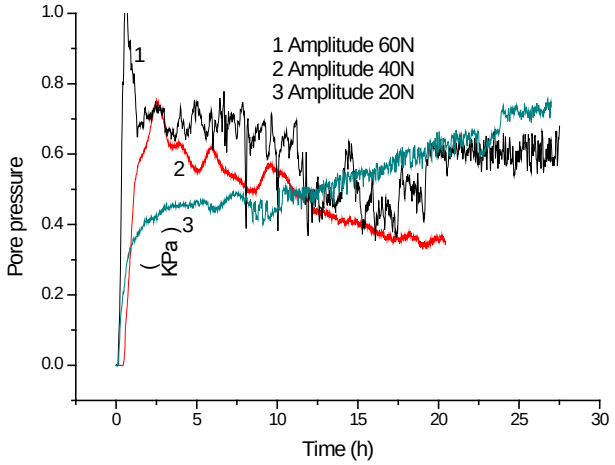

Fig. (2). Development of pore pressure under different load amplitude.

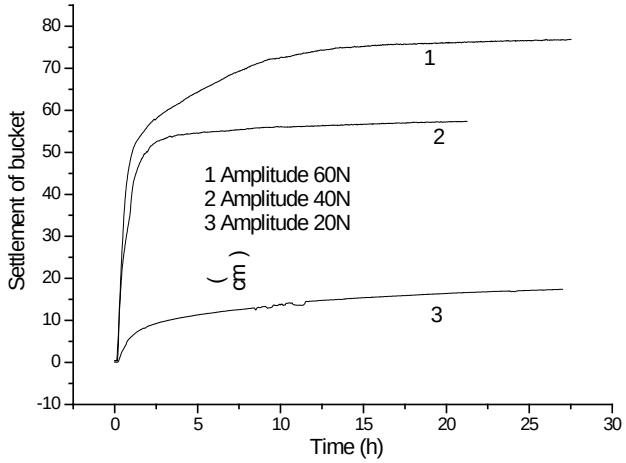

Fig. (3). Development of settlement of bucket under different load amplitude.

Fig. (4). Planform after experiments.

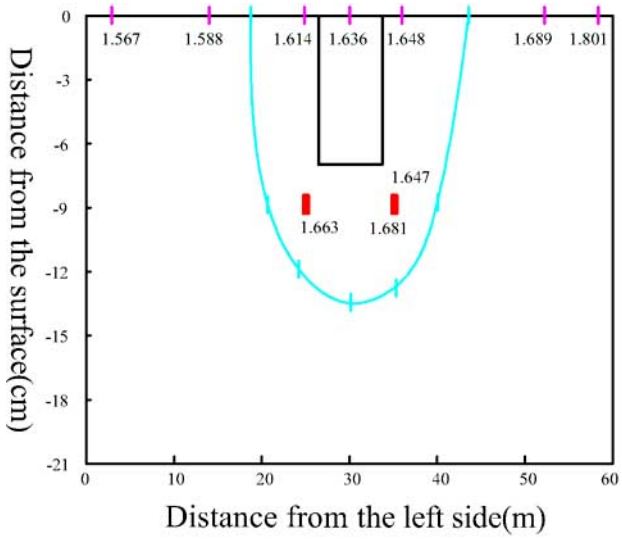

Fig. (5). Section of effects zone after an experiment.

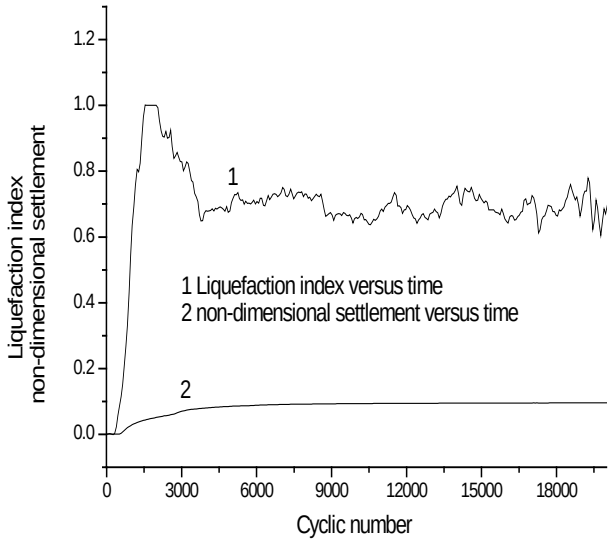

Fig. (6). The comparison of development of pore pressure and settlement of bucket.

CONCLUSIONS

Under the dynamic load with relative high frequency (such as 1.0Hz), the load cycle is a small value compared to the percolation time. That means, the inertial response is a fast process, while the percolation is a slow process. Therefore, the percolation and the inertial processes can be uncoupled. If we consider only the long-term responses but not the midcourse responses, the scalinng law of the percolation and the inertial need not be satisfied strictly and simultaneously when the load frequency is relatively large.

Main factors of bucket foundations are obtained by dimensionless analysis. A simplified method for the similarity simulation of permeability in centrifugal experiments is presented. The multi-scale asymptotic expansion method is used

to analyze the characteristic time and the characteristic scale of the affected zone of the soil layer surrounding the bucket foundation under long-term dynamic load.

REFERENCES

[1] E. C. Clukey, M. J. Morrison and J. Garnier, "The response of suction caissons in normally consolidated clays to cyclic TLP load conditions," In: *Proc. Offshore Tech. Conf.*, Houston, OTC 7796, 1995, pp. 909-918.

[2] H. G. B. Allersma, F. J. A. Plenevaux and J. F. P. C. M. E. Wintgens, "Simulation of suction pile installation in sand in a geocentrifuge," In: *Proc. 7th Int. Offshore Polar Eng. Conf.* (ISOPE97), Honolulu, Hawaii, USA, vol. 1, 1997, pp. 761-765.

[3] G. T. Housby and B. W. Byrne, "Suction caisson foundations for offshore wind turbines and anemometer masts," *Wind Eng.*, vol. 24, No. 4, pp. 249-255, 2000.

[4] B. W. Byrne, G. T. Housby, P. M. Fish and C. M. Martin, "Suction caisson foundations for offshore wind turbines", *Wind Eng.*, vol. 26, No. 3, pp. 145-155, 2002.

[5] B. W. Byrne and G. T. Housby, "Experimental investigations of the responses of suction caissons to transient combined load", *ASCE J. Geotech. Geoenviron. Eng.*, vol. 130, No. 3, pp. 240-253, 2004.

[6] K. H. Andersen and H. P. Jostad, "Foundation design of skirted foundations and anchors in clay," In: *Proc. Offshore Tech. Conf.*, Houston, Texas, OTC 10824, 1999, pp. 1-10.

[7] G. T. Housby and A. M. Puzrin, "A thermomechanical frame-work for constitutive models for rate-independent dissipative materials," *Int. J. Plasticity*, vol. 16, No. 9, pp. 1017-1047, 2000.

[8] D. Senpere and G. A. Auvergne, "Suction anchor piles-a proven alternative to driving or drilling," In: *Proc. Offshore Tech. Conf.*, Houston, OTC4206, 1982, pp. 483-493.

[9] P. M. Aas and K. H. Andersen, "Skirted foundation for offshore structure," In: *Proc. 9th Offshore South East Asia Conf.*, World Trade Center Singapore, 1992, pp. 1-7.

[10] W. Dyme and G. T. Housby, "Drained behavior of suction caisson on very dense sand," In: *Proc. Offshore Tech. Conf.*, Houston, OTC10994, 1998, pp. 765-782.

[11] T. L. Tjelta, J. Hermstad, and E. Andenaes, "The skirt piled gullfaks platform installation," In: *Proc. Offshore Tech. Conf.*, Houston, OTC6473, 1990, pp. 453-462.

[12] A. Bye, C. Erbrich, B. Rognlien and T.I. Tjelta, "Geotechnical design of bucket foundation," In: *Proc. Offshore Tech. Conf.*, Houston, OTC7793, 1995, pp. 869-883.

[13] R.N. Taylor, "Geotechnical centrifuge technology", Blackie Academic & Professional, London, 1995.

Received: July 18, 2008 Revised: August 20, 2009 Accepted: August 23, 2009